ORIGINAL PAPER

CrossMark

Cell-Type-Specific Spatiotemporal Expression of Creatine Biosynthetic Enzyme S-adenosylmethionine:guanidinoacetate *N*-methyltransferase in Developing Mouse Brain

Masanori Tachikawa[1,2] · Masahiko Watanabe[3] · Masahiro Fukaya[3] · Kazuhisa Sakai[3] · Tetsuya Terasaki[1] · Ken-ichi Hosoya[2]

Abstract

Creatine is synthesized by S-adenosylmethionine:guanidinoacetate *N*-methyltransferase (GAMT), and the creatine/phosphocreatine shuttle system mediated by creatine kinase (CK) is essential for storage and regeneration of high-energy phosphates in cells. Although the importance of this system in brain development is evidenced by the hereditary nature of creatine deficiency syndrome, the spatiotemporal cellular expression patterns of GAMT in developing brain remain unknown. Here we show that two waves of high GAMT expression occur in developing mouse brain. The first involves high expression in mitotic cells in the ventricular zone of the brain wall and the external granular layer of the cerebellum at the embryonic and neonatal stages. The second was initiated by striking up-regulation of GAMT in oligodendrocytes during the second and third postnatal weeks (i.e., the active myelination stage), which continued to adulthood. Distinct temporal patterns were also evident in other cell types. GAMT was highly expressed in perivascular pericytes and smooth muscle cells after birth, but not in adults. In neurons, GAMT levels were low to moderate in neuroblasts residing in the ventricular zone, increased during the second postnatal week when active dendritogenesis and synaptogenesis occur, and decreased to very low levels thereafter. Moderate levels were observed in astrocytes throughout development. The highly regulated, cell type-dependent expression of GAMT suggests that local creatine biosynthesis plays critical roles in certain phases of neural development. In accordance with this idea, we observed increased CK expression in differentiating neurons; this would increase creatine/phosphocreatine shuttle system activity, which might reflect increased energy demand.

Keywords Creatine · Developing brain · S-adenosylmethionine:guanidinoacetate *N*-methyltransferase · Biosynthesis · Creatine kinase

Abbreviations

BLBP	Brain-type lipid-binding protein
CK	Creatine kinase
CK-B	Brain-type cytoplasmic creatine kinase
GAMT	S-adenosylmethionine:guanidinoacetate *N*-methyltransferase
GFAP	Glial fibrillary acidic protein
GLUT	Glucose transporter
MAP	Microtubule associated protein
PLP	Proteolipid protein
SMA	Smooth muscle actin
uCK-Mi	Ubiquitous mitochondrial creatine kinase

✉ Masanori Tachikawa
tachik-dds@umin.ac.jp

1 Division of Membrane Transport and Drug Targeting, Graduate School of Pharmaceutical Sciences, Tohoku University, Sendai 980-8578, Japan

2 Department of Pharmaceutics, Graduate School of Medicine and Pharmaceutical Sciences, University of Toyama, Toyama, Japan

3 Department of Anatomy, Hokkaido University School of Medicine, Sapporo, Japan

Introduction

The creatine/phosphocreatine system is an intracellular energy shuttle catalyzed by creatine kinase (CK), and plays a crucial role in the storage and regeneration of high-energy phosphates in tissues with a high energy demand [1]. The physiological significance of this system is evidenced by the inherited disorder known as creatine deficiency syndrome, in which the main target is the brain of infants; patients exhibit

markedly decreased cerebral creatine levels and are afflicted with delayed psychomotor development, seizure and bilateral myelination delay [2, 3]. Therefore, creatine appears to be essential for normal neural development and function in infant brains. Creatine is supplied to the brain through two routes, i.e., transport from the circulation via the creatine transporter at the blood–brain barrier [4, 5] and local biosynthesis by S-adenosylmethionine:guanidinoacetate *N*-methyltransferase (GAMT) [5]. A case study of patients with GAMT deficiency, the first creatine deficiency syndrome to be discovered, indicated that oral creatine supplementation improves the neurological symptoms in part, but is insufficient to cure the disease [6], raising the possibility of the fundamental importance of local creatine biosynthesis in the brain.

We previously examined cellular expression of GAMT and CK in adult mouse brain [5]. GAMT is preferentially expressed in glial cells, including oligodendrocytes, astrocytes, and olfactory ensheathing glia, but its level in neurons is very low. Of the two CK isoforms in the brain, ubiquitous mitochondrial CK (uCK-Mi) is selectively expressed in neurons, whereas brain-type cytoplasmic CK (CK-B) is exclusively expressed in astrocytes among glial populations and in inhibitory neurons among neuronal populations. The distinct cellular expression patterns of GAMT and CKs suggest that creatine is mainly synthesized in glia and supplied to nearby neurons in the adult brain, and further imply that neurological symptoms in patients with GAMT deficiency could be ascribed, at least in part, to the effect of disrupted neuron-glial interplay on the creatine/phosphocreatine system. However, little is yet known about cellular expression of GAMT in the developing brain, although GAMT expression was reported to be low in embryonic rat brain [7]. In the present study, we aimed to clarify the spatiotemporal patterns of cellular expression of GAMT, as well as CKs, in developing mouse brain.

Materials and Methods

Animals and Section Preparation

Under deep pentobarbital anesthesia (100 mg/kg body, i.p.), brains of C57BL mice were obtained at embryonic day 13 (E13), E15, E18, postnatal day 1 (P1), P7, P10, P14, and P21. The day after overnight mating was counted as E0. For in situ hybridization, brains were freshly obtained and immediately frozen in powdered dry ice. Frozen sections (20 µm in thickness) were prepared on a cryostat (CM1900; Leica, Nussloch, Germany), mounted on silane-coated glass slides (Muto Pure Chemicals, Tokyo, Japan), and air-dried. For immunohistochemistry, postnatal brains were perfused transcardially with 4% paraformaldehyde in 0.1 M sodium phosphate buffer, pH 7.4, and processed for sectioning with a microslicer (50 µm, VT1000S; Leica). Investigations using mice conformed to the guidelines established by the Animal Care Committee, Tohoku University, University of Toyama, and Hokkaido University.

In Situ Hybridization

Antisense oligonucleotides were synthesized as probes for mouse GAMT, uCK-Mi, and CK-B mRNAs. The sequences corresponded to nucleotide residues 111–155 and 750–794 of mouse GAMT (GenBank accession number NM_010255), 45–89 of mouse CK-B (NM_021273), and 122–167 of mouse uCK-Mi (BC025976). Probe labeling with [^{33}P]dATP, pre-hybridization, hybridization, washing, and autoradiography were carried out as reported previously [8]. For nonisotopic detection, a digoxigenin-labelled antisense cRNA probe was used to detect mouse proteolipid protein (PLP) mRNA with a 2-hydroxy-3-naphthoic acid-2-phenylanilide phosphate fluorescence detection set (Roche Molecular Biochemicals, Mannheim, Germany), as reported [5].

Immunohistochemistry

For immunofluorescence studies, sections were incubated at room temperature with 10% normal donkey serum for 30 min, guinea pig anti-GAMT antibody (2 µg/mL) [5] alone or in combination with rabbit anti-microtubule associated protein (MAP) 2 antiserum (1:5000) [5], rabbit anti-brain-type lipid-binding protein (BLBP) antibody (1 µg/mL) [9], rabbit anti-glucose transporter 1 (GLUT1) antibody (0.5 µg/mL) [10], rabbit anti-calbindin antibody (1:5000) [11], mouse anti-α-smooth muscle actin (SMA) antibody (1:100, American Research Products, Belmont, MA, USA), or rabbit glial fibrillary acidic protein (GFAP) antibody (DAKO, Carpinteria, CA, USA). Then, the sections were incubated with species-specific FITC-, indocarbocyanine (Cy3)- and indodicarbocyanine (Cy5)-conjugated secondary antibodies for 2 h (Jackson ImmunoResearch, West Grove, PA, USA). Photographs were taken using a confocal laser-scanning microscope (Fluoview, Olympus, Tokyo, Japan). Immunoperoxidase electron microscopy was performed as reported previously [5]. Briefly, microslicer sections processed for immunoperoxidase were treated with 1% osmium tetroxide for 15 min and 2% uranyl acetate for 30 min, dehydrated using graded alcohols and embedded in Epon 812. All electron micrographs were taken using an H-7100 electron microscope (Hitachi, Tokyo, Japan).

Results

GAMT mRNA Expression in Developing Brains

The spatiotemporal expression patterns of GAMT mRNA in mouse brain were examined from E13 to P21 by means of in situ hybridization with ^{33}P-labeled antisense probes (Fig. 1). The specificity of the detected signals was verified by the observation of identical patterns with two non-overlapping probes, and by the absence of signals when hybridization was carried out in the presence of an excess of unlabeled probes (data not shown).

During embryonic stages, high to moderate levels of GAMT mRNA were detected in the ventricular zone, a germinal zone producing neurons, astrocytes, and oligodendrocytes, in various brain regions (Fig. 1a–c). Prominent signals also appeared in the external granular layer of the cerebellum, a germinal zone producing cerebellar granule cells, at E18 and peaked at P7-P10 (Fig. 1c–f). Signals in these germinal zones diminished thereafter, as the zones disappeared during the course of development. Low and moderate signals appeared in the gray matter and white matter at around birth (Fig. 1c, d), and the levels in the white matter, such as the corpus callosum and cerebellar medulla, markedly increased toward P14 (Fig. 1d–h). Laminar expression in the gray matter of the cerebral cortex and hippocampus was seen at P7 and P10 (Fig. 1e, f), but became obscure by P14 and P21 (Fig. 1g, h).

Cellular Expression of GAMT at P1

Cellular expression of GAMT was examined in early postnatal brains by means of immunofluorescence studies (Figs. 2, 3). At P1, intense immunostaining of GAMT was detected in the ventricular zone of the brain wall (Fig. 2a, b) and the external granular layer of the cerebellum (Fig. 2h, i). We used BLBP and MAP2 as cellular markers for the neural stem cell/radial glia/astrocyte lineage and the neuroblast/neuron lineage, respectively. In the ventricular zone, GAMT was detected in both BLBP-positive neural stem cells/radial glia and BLBP-negative neuroblasts (Fig. 2b). In the cortical plate, moderately intense GAMT staining was seen in BLBP-positive somata and processes of radial glia/astrocytes (arrowheads in Fig. 2c, f). Weak GAMT staining was detected in MAP2-positive neuronal somata and dendrites (Fig. 2g). In the cerebellar cortex, GAMT was expressed in BLBP-positive astrocytes, i.e., prospective Bergmann glia and common astrocytes, and in BLBP-negative external granule cells (Fig. 2i).

Intense signals of GAMT were also detected in BLBP-negative circular or cylindrical profiles of blood vessels (Fig. 2a, b, arrowheads). GAMT-expressing vessels were often associated with BLBP-positive/GAMT-positive perivascular astrocytes (Fig. 2c, arrowheads). Comparison with the signals of GLUT1, a marker of vascular endothelial cells, and α-SMA, a marker of smooth muscle cells and pericytes, showed that GAMT was selectively expressed in α-SMA-positive pericytes, but not GLUT1-positive endothelial cells, in thin vessels (Fig. 2d, e, arrows). It should be noted that a 45-kDa isoform of GLUT1 protein, which is different from the 55-kDa microvessel-type isoform of GLUT1 protein, is expressed in astrocytes and oligodendrocytes [12]. However, we have reported that immunostaining for ABCG2, which showed selective localization in brain capillary endothelial cells as determined by immuno-electron microscopy, overlaps with that of GLUT1 [8]. This indicated the antibody used in the present study predominantly recognizes the microvessel-type isoform of GLUT1. On the surface of the brain, GAMT was also detected in BLBP-negative (Fig. 2f, asterisks) and GLUT1-negative (data not shown) blood vessels (Fig. 2a, asterisks), suggesting its possible expression in smooth muscle cells associated with arteries and arterioles.

Cellular Expression of GAMT at P7-P14

As shown in Fig. 3a, b, GAMT immunoreactivity was widely detected in the cerebral cortex, corpus callosum, and hippocampus at P7 and P10. The only major difference between the two postnatal stages was intensified labeling in the corpus callosum at P10 (Fig. 3a, b, arrowheads). Small cells strongly labeled for GAMT were scattered in these regions (Fig. 3c–f, arrowheads); they were BLBP-positive astrocytes often attached to GLUT1-positive vascular endothelial cells (Fig. 3c, arrowheads). Immunoelectron microscopy showed intense staining in astrocytic processes surrounding synapses (Fig. 4a). Occasionally, we also encountered GAMT-positive pericytes attached to endothelial cells, which were negative for BLBP or GLUT1 (Fig. 3c, arrows), but positive for α-SMA (data not shown). Laminar distribution of GAMT immunoreactivity was noted in the cerebral cortex at P7-P10, with higher levels in layers I and IV. Double immunofluorescence staining for GAMT and MAP2 showed that neuronal perikarya and dendrites were positive for GAMT (Fig. 3d). Immunoelectron microscopy showed moderate staining in dendritic spines forming asymmetrical synapses (Fig. 4a, b, asterisks).

In the corpus callosum at P7, GAMT staining was intense in GFAP-positive astrocytes (Fig. 3e, arrowheads) and moderate in GFAP-negative cells (Fig. 3e, arrows). The intensity in GFAP-negative cells was remarkably increased at P10 (Fig. 3f, arrows); these cells appeared to be oligodendrocytes expressing mRNA for PLP, a myelin-specific protein (Fig. 3g, arrows). In the cerebellum at P10, intense
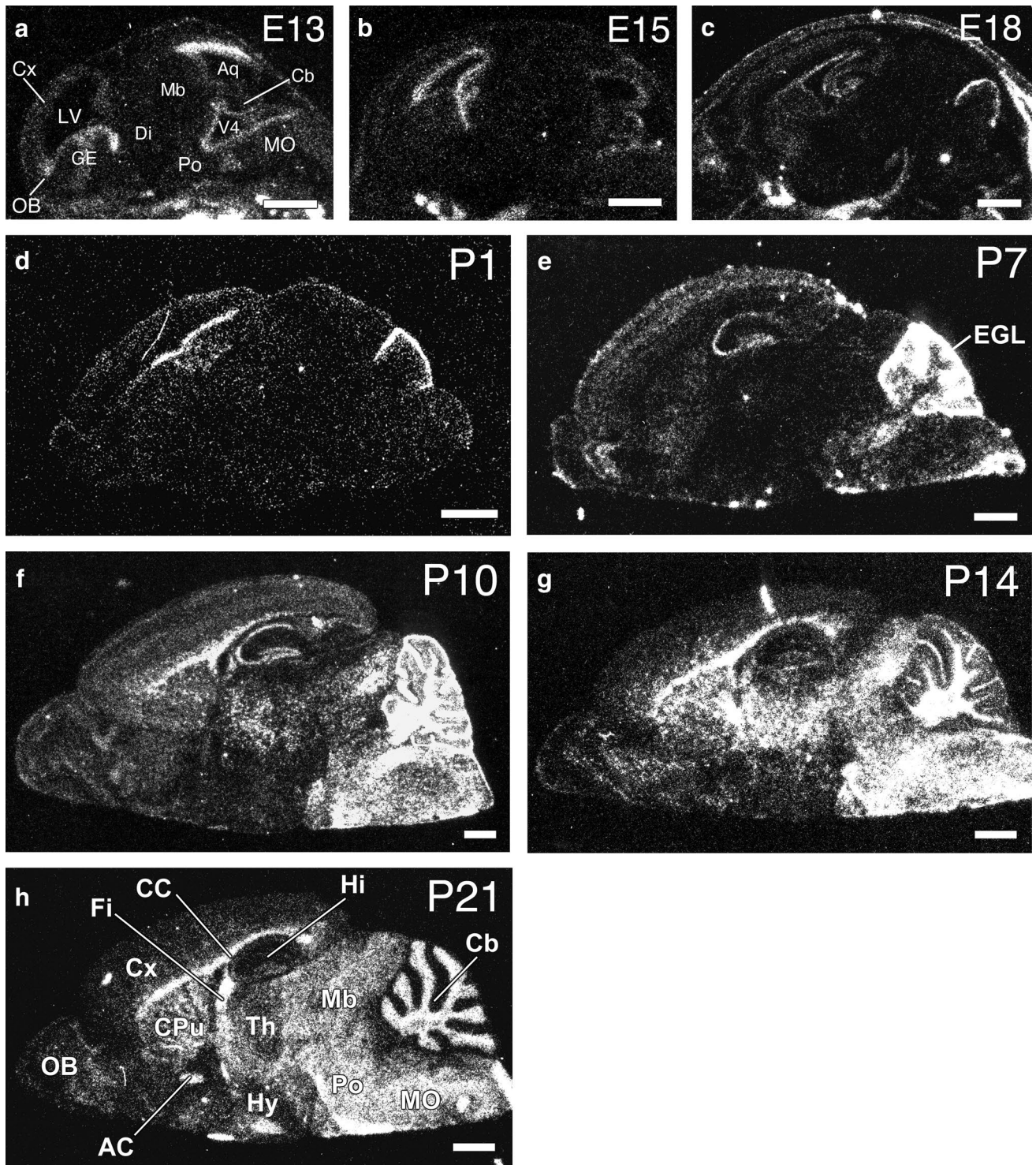
Fig. 1 Detection of GAMT mRNA in developing mouse brain by in situ hybridization. Negative images were made from X-ray film autoradiograms of parasagittal brain sections at E13 (**a**), E15 (**b**), E18 (**c**), P1 (**d**), P7 (**e**), P10 (**f**), P14 (**g**), and P21 (**h**). *AC* anterior commissure, *Aq* cerebral aqueduct, *Cb* cerebellum, *CC* corpus callosum, *CPu* caudate-putamen, *Cx* cerebral cortex, *Di* diencephalon, *EGL* external granular layer, *Fi* fimbria, *GE* ganglionic eminence, *Hi* hippocampus, *Hy* hypothalamus, *LV* lateral ventricle, *Mb* midbrain, *MO* medulla oblongata, *OB* olfactory bulb, *Po* pons, *Th* thalamus, *V4* fourth ventricle. Scale bars—1 mm
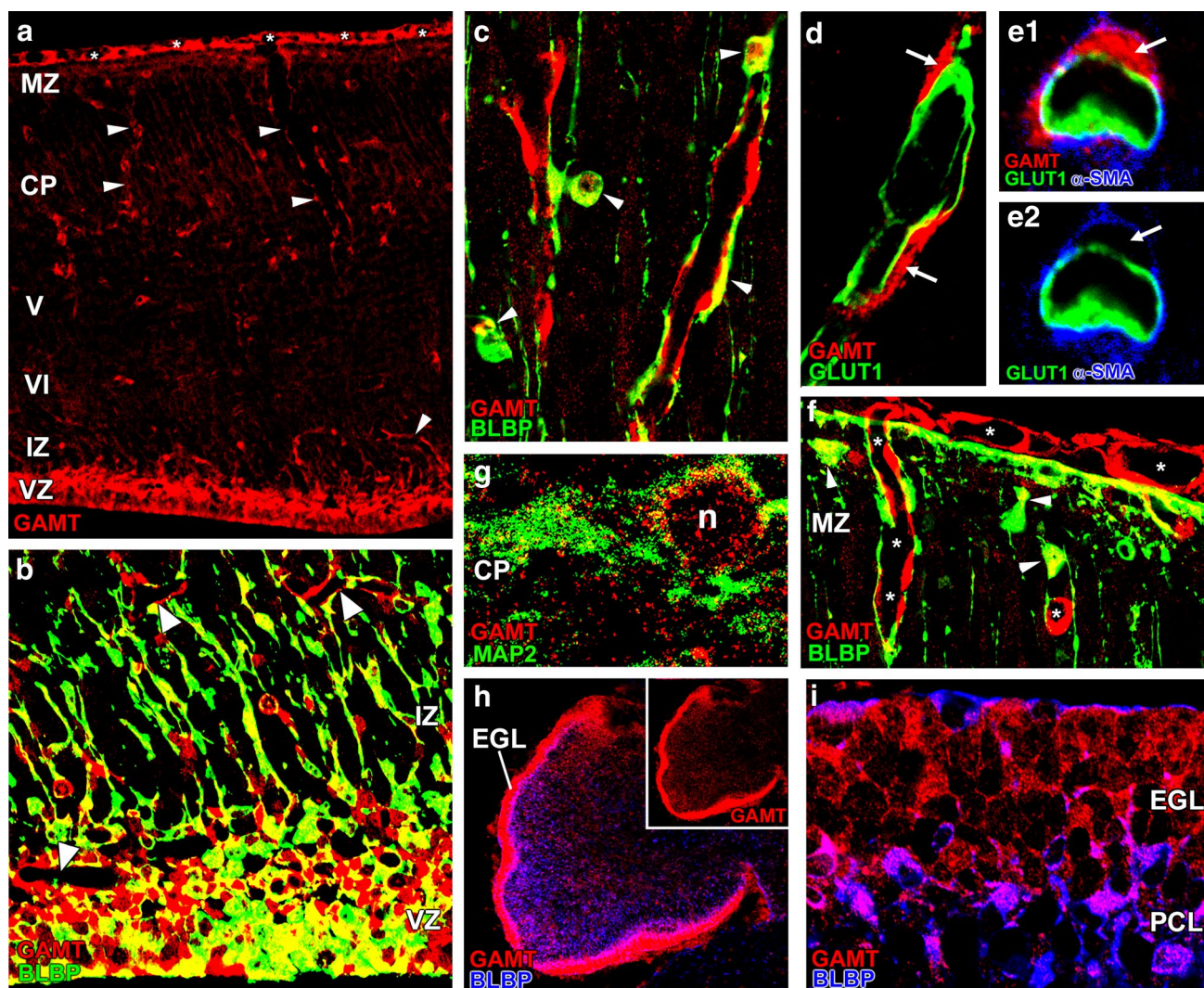
Fig. 2 Immunofluorescence staining of GAMT in mouse neocortex (**a–g**) and cerebellum (**h, i**) at P1. In all images, GAMT is in red. Green fluorescence and blue fluorescence are defined at the lower left corner of each panel. **a** GAMT immunofluorescence in the neocortex. Note the high levels of GAMT in the ventricular zone (VZ) and on the surface of the neocortex (asterisks). Also note intense GAMT expression in vessel-like structures (arrowheads) and moderate levels of GAMT in the cortical plate (CP). *IZ* intermediate zone, *MZ* marginal zone, *V and VI* cortical layers V and VI. **b** High expression of GAMT in BLBP-labeled neuroepithelial or neural precursor cells in the ventricular zone. Arrowheads indicate vessel-like structures. *IZ* intermediate zone. **c** Expression of GAMT in BLBP-labeled glial cells (arrowheads) in the cortical plate. **d** Lack of GAMT expression in GLUT1-positive vessel endothelial cells in the cortical plate.

Note that cells strongly expressing GAMT (arrows) are associated with GLUT-positive endothelial cells. **e** Triple immunofluorescence for GAMT, GLUT1, and α-SMA in the cortical plate. GAMT is expressed in α-SMA-positive pericytes (arrows) but not in GLUT1-positive endothelial cells. **f** Expression of GAMT in BLBP-labeled glial cells (arrowheads). Note intense GAMT expression in vessel-like structures (asterisks) on BLBP-labeled glial limitations and within the marginal zone (MZ). **g** Expression of GAMT in MAP2-positive neuron (n) in the cortical plate (CP). **h** and **i** High expression of GAMT in the external granular layer (EGL) and in BLBP-labeled glial cells in the cerebellum. Inset in **h**; single staining of GAMT. *PCL* Purkinje cell layer. Scale bars—10 μm (**a–g, i**), 50 μm (**h**). (Color figure online)

labeling for GAMT was maintained in the external granule cells, and GFAP-positive astrocytes having radial fibers, i.e., Bergmann glia, were seen (Fig. 3h, i, arrowheads). Double immunofluorescence staining for GAMT and calbindin, a cytosolic protein rich in Purkinje cells, showed that GAMT levels were low to moderate in cell bodies and shaft dendrites of Purkinje cells (Fig. 3i).

At P14, intense GAMT staining was maintained in BLBP-positive astrocytes (Fig. 3j, k, arrowheads) and BLBP-negative oligodendrocytes (Fig. 3k, arrow), but had almost disappeared from pericytes (Fig. 3j, arrow) in the cerebral cortex and corpus callosum. In neurons, GAMT staining was decreased to very low levels in the cerebral cortex (data not shown).
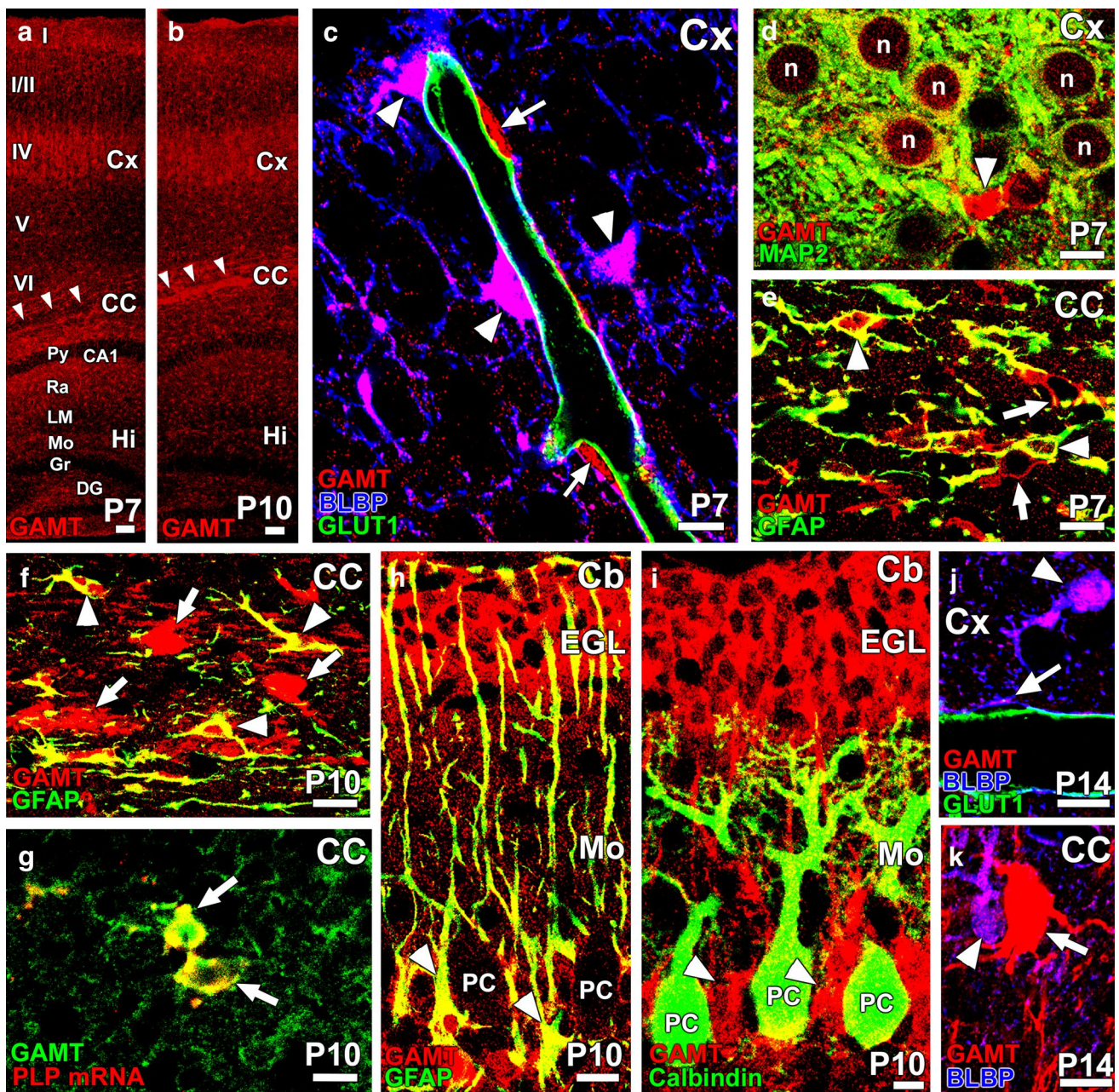
Fig. 3 Cellular expression of GAMT in mouse brain at P7 (**a, c–e**), P10 (**b, f–i**), and P14 (**j, k**). Red, blue, and green fluorescence is defined at the lower left corner of each panel. **a, b** Comparison of GAMT immunofluorescence in the cerebral cortex (Cx), corpus callosum (CC), and hippocampus (Hi) at P7 (**a**) and P10 (**b**). Arrowheads indicate the labeling in the corpus callosum. *CA1* CA1 region of Ammon's horn, *DG* dentate gyrus, *Gr* granular layer, *LM* stratum lacunosum-moleculare, *Mo* molecular layer, *Py* pyramidal cell layer, *Ra* stratum radiatum, *I-VI* laminas I-VI of the cerebral cortex. **c** High expression of GAMT in BLBP-positive astrocytes (arrowheads) and lack of GAMT in GLUT1-positive microvessels in the cerebral cortex (Cx). Arrows indicate both BLBP- and GLUT1-negative cells associated with microvessels. **d** Expression of GAMT in MAP2-positive neurons (n) in the cerebral cortex (Cx). Arrowhead indicates MAP2-negative small cells strongly expressing GAMT. **e, f** High expression of GAMT in GFAP-positive astrocytes (arrowheads) in corpus cal-losum (CC). Note the marked upregulation of GAMT expression in GFAP-negative cells (arrows) at P10. **g** High expression of GAMT in PLP mRNA-positive oligodendrocytes (arrows) in corpus callosum (CC). **h** Intense GAMT expression in GFAP-positive Bergmann glia (arrowheads) in cerebellum (Cb). *EGL* external granular layer, *Mo* molecular layer, *PC* Purkinje cell. **i** Moderate staining of GAMT in calbindin-positive Purkinje cells (PC) in cerebellum (Cb). Arrowheads indicate GAMT-expressing cell bodies of Bergmann glia. Note intense GAMT expression in the external granular layer (EGL). *Mo* molecular layer. **j** Expression of GAMT in BLBP-positive astrocytes (arrowhead) in cerebral cortex (Cx) and lack of GAMT expression in cells (arrow) associated with GLUT1-positive microvessels. **k** Expression of GAMT in BLBP-positive astrocytes (arrowhead) and BLBP-negative oligodendrocytes (arrow) in the corpus callosum (CC). Scale bars—10 µm. (Color figure online)
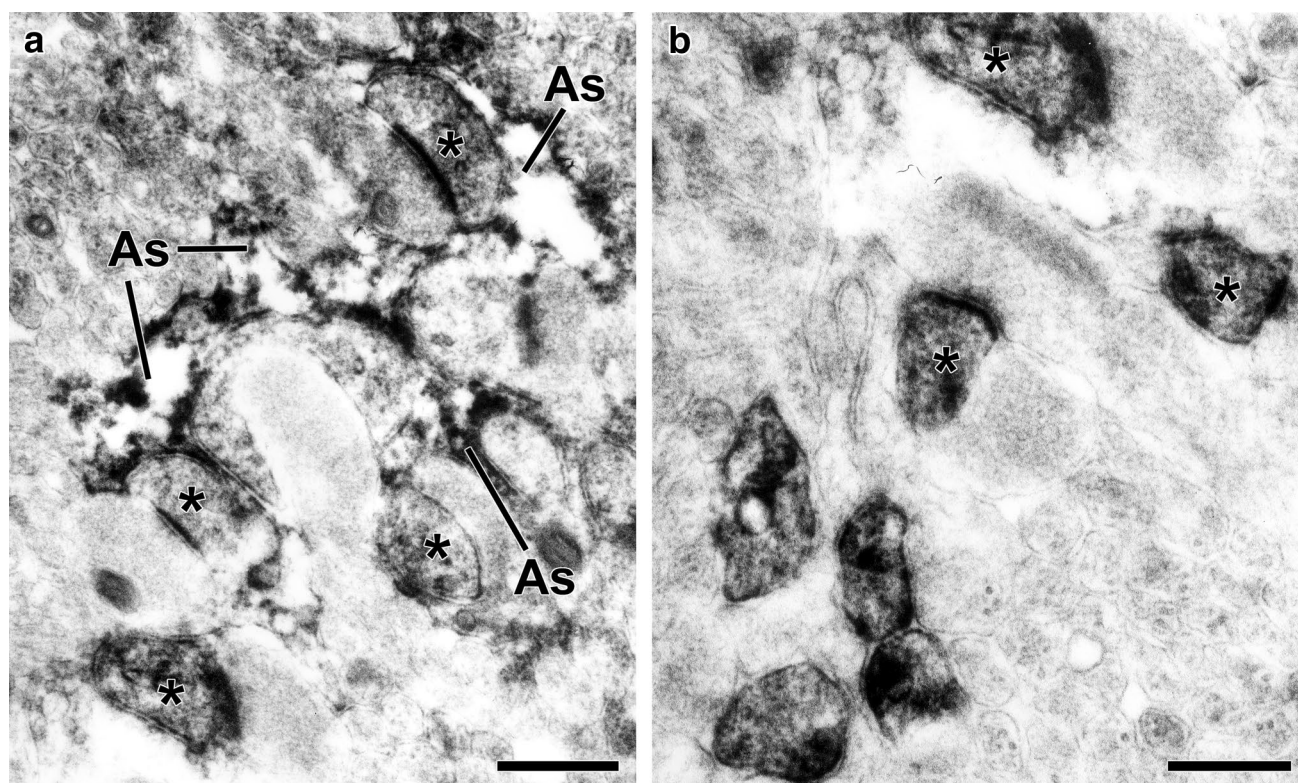
Fig. 4 Immunoperoxidase electron microscopy for GAMT in the cerebral cortex at P10. Note intense immunolabeling in dendritic spines of neurons (**a, b**) and astrocytic processes (As, **a**) surrounding synapses. Asterisks represent the dendritic spines forming asymmetrical synapses. Scale bars—0.5 µm

Developmental Changes in Expression of uCK-Mi and CK-B mRNAs

Spatiotemporal changes in expression of uCK-Mi and CK-B mRNAs were examined in developing mouse brains by means of in situ hybridization with ^{33}P-labeled antisense probes (Figs. 5, 6). The detection specificity of uCK-Mi and CK-B mRNAs was verified by the absence of signals when hybridization was carried out in the presence of an excess of unlabeled probe (data not shown).

uCK-Mi mRNA level was generally low in embryonic brain (Fig. 5a–c). Faint signals were detected in the mantle zone of various brain regions, such as the cortical plate at E15 and E18, while no significant signal was found in the ventricular zone (Fig. 5b, c). After birth, uCK-Mi mRNA was markedly up-regulated throughout the gray matter of the brain, showing laminar patterns in the olfactory bulb, cerebral cortex, hippocampus and cerebellar cortex, and nucleus-related patterns in the basal ganglia and brainstem, suggestive of neuronal expression (Fig. 5d–f). No signal was detected in the external granular layer of the cerebellum (Fig. 5d, e).

In contrast, high levels of CK-B mRNA were detected in various regions of embryonic brain, with higher levels in the ventricular zone than in the mantle zone (Fig. 6a–c). After birth, intense, widespread expression in the brain continued until P21, the last postnatal stage examined (Fig. 6d–f). It is noteworthy that CK-B transcripts not only showed discrete laminar or nucleus-related patterns in the gray matter, but also exhibited diffuse labeling in the white matter and intense expression in the external granular layer of the cerebellum. These distinct expression profiles may reflect different cellular expression patterns of uCK-Mi and CK-B, both spatially and temporally.

Discussion

Our present findings indicate that GAMT shows two waves of expression in developing mouse brain: the first wave occurs in the ventricular zone at the embryonic and neonatal stages, and the second wave occurs in the gray matter and white matter during the second and third postnatal weeks (Table 1). We also observed distinct spatiotemporal expression patterns of uCK-Mi and CK-B mRNAs in developing brain (Table 1). Further studies will be needed to evaluate the functional contribution of GAMT to the CK-mediated
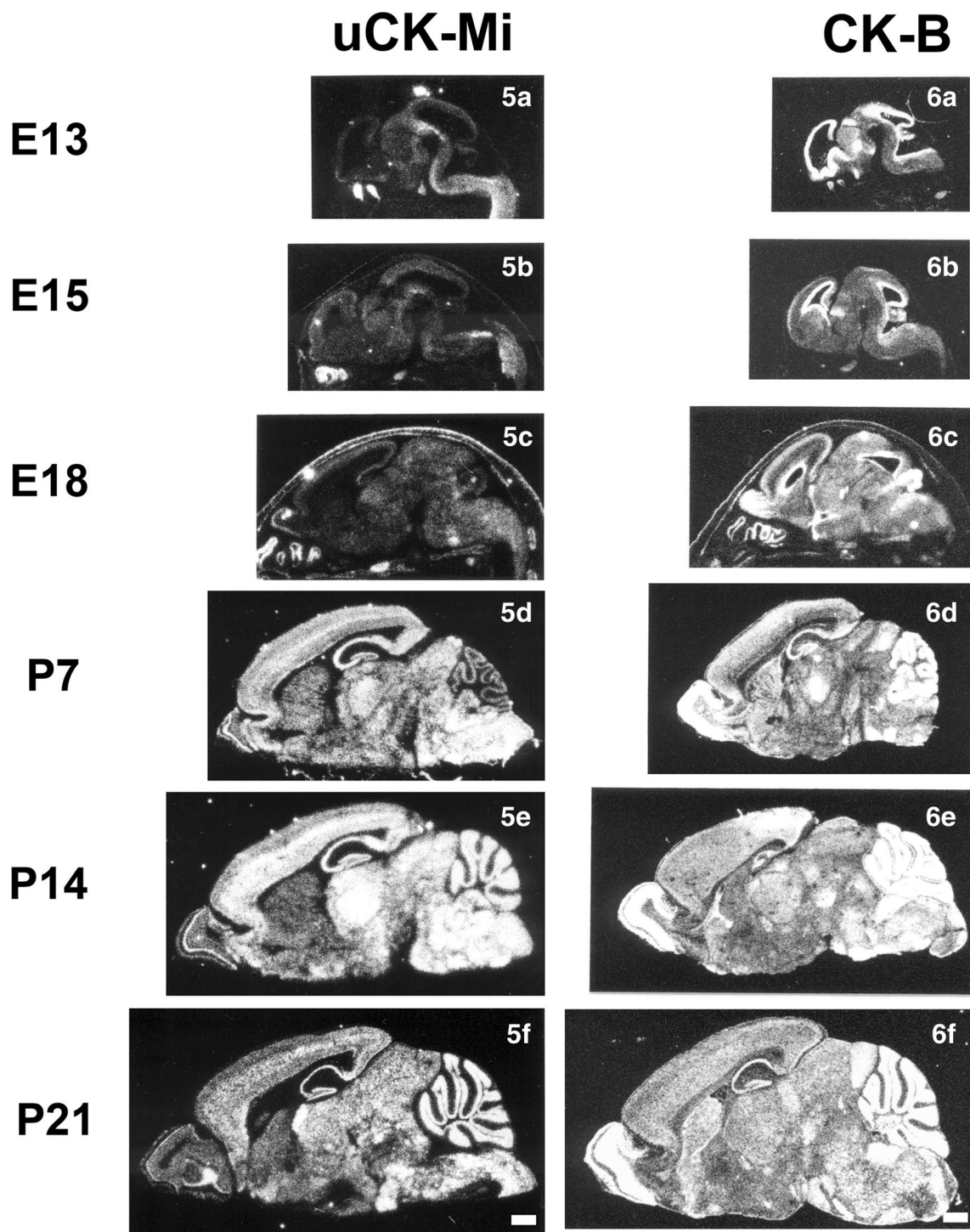
Figs. 5 and 6 Detection of uCK-Mi mRNA (Fig. 5) and CK-B (Fig. 6) in developing mouse brain by in situ hybridization. Negative images were made from X-ray film autoradiograms of parasagittal brain sections at E13 (**a**), E15 (**b**), E18 (**c**), P7 (**d**), P14 (**e**), P21 (**f**). Brain regions and abbreviations are shown in Fig. 1. Scale bars—1 mm

creatine/phosphocreatine shuttle in the developing brain, for example by using cell-type specific and time-controlled gene knockout mice.

GAMT in Neural Progenitors

High GAMT expression was detected in neural stem cells constituting the ventricular zone, and also in the external

Table 1 Cellular expression profiles of GAMT, uCK-Mi, and CK-B in the postnatal mouse brains

	P1	P7	P10	P14	P21
GAMT mRNA/protein					
Neuroblast/neuron lineage	+	++	++~+	+	+
Neural stem cells/radial glia/astrocyte lineage	+	++	++	++	++
Oligodendrocyte		+	++	++	++
Pericyte/smooth muscle cell	++	++	+	−	−
Endothelial cell	−	−	−	−	−
uCK-Mi mRNA					
Neuroblast/neuron lineage	+	+	+	+	+
Neural stem cells/radial glia/astrocyte lineage	−	−	−	−	−
CK-B mRNA					
Neuroblast/neuron lineage	+	+	+	+	+
Neural stem cells/radial glia/astrocyte lineage	+	+	+	+	+

Cellular expression of GAMT mRNA/protein is shown based on the results in Figs. 1, 2, and 3 (− represents no expression, + represents low to moderate expression, ++ represents strong expression). Suggested cellular expressions of uCK-Mi and CK-B mRNAs are shown based on the results in Figs. 5 and 6 (− represents no expression, + represents positive expression)

granular layer. This expression profile suggests enhanced demand for creatine biosynthesis in mitotic cells that produce prospective neurons and glia. During cell division, microtubule motors driving spindle elongation in the anaphase require ATP, which is provided by CK [13, 14]. Involvement of CK-B in cell division has been inferred from its elevated activity and immunoreactivity in proliferating astrocytes compared with non-proliferating astrocytes [15]. It is interesting that both CK-B and GAMT mRNAs were highly expressed in these proliferative zones. Considering that CK is essential for reversible exchange of a high-energy phosphoryl group between phosphocreatine and ATP, it can be assumed that GAMT and CK-B are up-regulated in neural progenitor cells to meet the elevated demand for creatine-mediated transfer and storage of high-energy phosphates and for rapid repletion of cytosolic ATP to support the active cell cycle.

GAMT in Oligodendrocytes

Elevated GAMT expression in the second and third postnatal weeks was mainly ascribed to up-regulation in PLP mRNA-positive oligodendrocytes. Expression of various myelin-specific genes is also elevated during this period [16, 17]. Thus, GAMT up-regulation could be taken as reflecting the increased requirement for creatine in myelinating oligodendrocytes. Low and diffuse expression of CK-B mRNA in the white matter, as well as cytosolic CK activity in cultured oligodendrocytes [18], may reflect the function of the creatine/phosphocreatine shuttle system in energy homeostasis.

Nevertheless, expression of GAMT far surpassed that of CK-B and uCK-Mi mRNAs during the active myelination stage. Such a discrepancy is even more evident in adulthood, when the highest level of GAMT expression is found in oligodendrocytes, whereas CK-B and uCK-Mi expression is below the detection threshold [5]. These findings raise the possibility that oligodendrocytes may synthesize creatine not only for their own use, but also for transfer to neighboring cells, if CK activity is rate-limiting in the GAMT-CK pathway. It has been reported that glia-derived creatine is involved in axon growth [19], and neuronal CK promotes axon elongation and growth cone activity [20]. Our previous study demonstrated that uCK-Mi is predominantly expressed in neuronal cell populations, in which it is selectively localized in mitochondria [5]. The present observation of laminar and nucleus-related patterns of uCK-Mi mRNA expression (Fig. 5) supports neuronal expression in early postnatal brains. Given ample phosphocreatine, the creatine/phosphocreatine shuttle system can generate ATP at rates 10 times faster than oxidative phosphorylation and 40 times faster than glycolysis [21]. It is an intriguing possibility that axonal creatine is supplied, at least in part, by local oligodendrocytes that enwrap the axons. This might also be the case in olfactory ensheathing glia, a specialized supporting cell type that enwraps olfactory nerves; these cells also express the highest level of GAMT in adult brains, but lack detectable levels of CK-B or uCK-Mi [5].

GAMT in Perivascular Cells

It was unexpected to find high expression of GAMT in pericytes and smooth muscle cells at P1-P10. This is a transient phenomenon, because it is not observed in adult brains [5]. Smooth muscle cells and pericytes regulate the constriction and dilation of arteries, arterioles, and capillaries, regulating the cerebral blood flow [22]. In smooth muscle cells, CK is localized at sites of ATP utilization and production, and functions as an integral component of muscle contraction

[23]. Thus, this transient expression suggests active creatine biosynthesis to meet energy demands for active control of cerebral blood flow, and also to supply creatine to differentiating capillaries and/or brain parenchyma. After down-regulation of GAMT, capillaries in adult brains may participate in transport of blood-borne creatine to the brain parenchyma, as reported previously [1, 4, 24].

GAMT in Neurons and Astrocytes

GAMT-expressing cells in the ventricular zone included both BLBP-positive cells, i.e., cells in the neural stem cells/radial glia/astrocyte lineage, and BLBP-negative cells, i.e., cells in the neuroblast/neuronal lineage. This was confirmed during the early postnatal period by the observation of low to moderate GAMT immunoreactivity in BLBP-positive perivascular astrocytes and GFAP-positive Bergmann glia, and in MAP2-positive cortical neurons and calbindin-positive Purkinje cells. GAMT expression in astrocytes was well maintained until adulthood [5], whereas the expression in neurons decreased as the brain matured [5].

Neuronal GAMT expression was elevated at P7-P10, when a laminar pattern of GAMT expression was clearly observed, and immunoelectron microscopy revealed the presence of GAMT in dendritic spines of cortical neurons. During this period, cortical neurons display active dendritogenesis and synaptogenesis, and CK serves to meet neuronal energy requirements during synaptogenesis [25, 26] and overall neuronal growth [27]. Thereafter, GAMT expression decreased to very low levels in neurons or in the gray matter (Fig. 1). Therefore, differentiating neurons have not only high capacity for creatine biosynthesis, but also have access to various sources of exogenous creatine from the circulation and neighboring cells (oligodendrocytes, astrocytes, pericytes, and smooth muscle cells). High levels of CK, particularly uCK-Mi, in neurons further suggest that neurons can efficiently drive the creatine/phosphocreatine energy shuttle system if a sufficient supply of creatine is available.

In conclusion, GAMT and CKs exhibit drastic changes in spatiotemporal expression in the developing brain. This suggests availability of large amounts of locally biosynthesized creatine as well as high demand for the creatine/phosphocreatine energy shuttle system in cell type-specific and time-controlled manners. This idea is consistent with the appearance of severe neurological symptoms in infants with inherited creatine deficiency syndrome.

Compliance with Ethical Standards

Conflict of interest The authors have no conflict of interest to declare.

References

1. Wyss M, Kaddurah-Daouk R (2000) Creatine and creatinine metabolism. Physiol Rev 80:1107–1213
2. Salomons GS, van Dooren SJ, Verhoeven NM, Marsden D, Schwartz C, Cecil KM, DeGrauw TJ, Jakobs C (2003) X-linked creatine transporter defect: an overview. J Inherit Metab Dis 26:309–318
3. Stromberger C, Bodamer OA, Stockler-Ipsiroglu S (2003) Clinical characteristics and diagnostic clues in inborn errors of creatine metabolism. J Inherit Metab Dis 26:299–308
4. Ohtsuki S, Tachikawa M, Takanaga H, Shimizu H, Watanabe M, Hosoya K, Terasaki T (2002) The blood-brain barrier creatine transporter is a major pathway for supplying creatine to the brain. J Cereb Blood Flow Metab 22:1327–1335
5. Tachikawa M, Fukaya M, Terasaki T, Ohtsuki S, Watanabe M (2004) Distinct cellular expressions of creatine synthetic enzyme GAMT and creatine kinases uCK-Mi and CK-B suggest a novel neuron-glial relationship for brain energy homeostasis. Eur J Neurosci 20:144–160
6. Stöckler S, Isbrandt D, Hanefeld F, Schmidt B, von Figura K (1996) Guanidinoacetate methyltransferase deficiency: the first inborn error of creatine metabolism in man. Am J Hum Genet 58:914–922
7. Braissant O, Henry H, Villard AM, Speer O, Wallimann T, Bachmann C (2005) Creatine synthesis and transport during rat embryogenesis: spatiotemporal expression of AGAT, GAMT and CT1. BMC Dev Biol 5:9
8. Tachikawa M, Watanabe M, Hori S, Fukaya M, Ohtsuki S, Asashima T, Terasaki T (2005) Distinct spatio-temporal expression of ABCA and ABCG transporters in the developing and adult mouse brain. J Neurochem 95:294–304
9. Yamada K, Fukaya M, Shibata T, Kurihara H, Tanaka K, Inoue Y, Watanabe M (2000) Dynamic transformation of Bergmann glial fibers proceeds in correlation with dendritic outgrowth and synapse formation of cerebellar Purkinje cells. J Comp Neurol 418:106–120
10. Sakai K, Shimizu H, Koike T, Furuya S, Watanabe M (2003) Neutral amino acid transporter ASCT1 is preferentially expressed in L-Ser-synthetic/storing glial cells in the mouse brain with transient expression in developing capillaries. J Neurosci 23:550–560
11. Nakagawa S, Watanabe M, Isobe T, Kondo H, Inoue Y (1998) Cytological compartmentalization in the staggerer cerebellum, as revealed by calbindin immunohistochemistry for Purkinje cells. J Comp Neurol 395:112–120
12. Yu S, Ding WG (1998) The 45 kDa form of glucose transporter 1 (GLUT1) is localized in oligodendrocyte and astrocyte but not in microglia in the rat brain. Brain Res 797:65–72
13. Cande WZ (1983) Creatine kinase role in anaphase chromosome movement. Nature 304:557–558
14. Koons SJ, Eckert BS, Zobel CR (1982) Immunofluorescence and inhibitor studies on creatine kinase and mitosis. Exp Cell Res 140:401–409
15. Manos P, Bryan GK (1993) Cellular and subcellular compartmentation of creatine kinase in brain. Dev Neurosci 15:271–279
16. Kanfer J, Parenty M, Goujet-Zalc C, Monge M, Bernier L, Campagnoni AT, Dautigny A, Zalc B (1989) Developmental expression of myelin proteolipid, basic protein, and 2′,3′-cyclic

nucleotide 3′-phosphodiesterase transcripts in different rat brain regions. J Mol Neurosci 1:39–46

17. Sorg BA, Smith MM, Campagnoni AT (1987) Developmental expression of the myelin proteolipid protein and basic protein mRNAs in normal and dysmyelinating mutant mice. J Neurochem 49:1146–1154

18. Manos P, Bryan GK, Edmond J (1991) Creatine kinase activity in postnatal rat brain development and in cultured neurons, astrocytes, and oligodendrocytes. J Neurochem 56:2101–2107

19. Braissant O, Henry H, Villard AM, Zurich MG, Loup M, Eilers B, Parlascino G, Matter E, Boulat O, Honegger P, Bachmann C (2002) Ammonium-induced impairment of axonal growth is prevented through glial creatine. J Neurosci 22:9810–9820

20. Wang YE, Esbensen P, Bentley D (1998) Arginine kinase expression and localization in growth cone migration. J Neurosci 18:987–998

21. Wallimann T, Wyss M, Brdiczka D, Nicolay K, Eppenberger HM (1992) Intracellular compartmentation, structure and function of creatine kinase isoenzymes in tissues with high and fluctuating energy demands: the 'phosphocreatine circuit' for cellular energy homeostasis. Biochem J 281(Pt 1):21–40

22. Peppiatt CM, Howarth C, Mobbs P, Attwell D (2006) Bidirectional control of CNS capillary diameter by pericytes. Nature 443:700–704

23. Clark JF (1994) The creatine kinase system in smooth muscle. Mol Cell Biochem 133–134:221–232

24. Walker JB (1979) Creatine: biosynthesis, regulation, and function. Adv Enzymol Relat Areas Mol Biol 50:177–242

25. Lapin EP, Maker HS, Lehrer GM (1974) Changes during development of mouse brain in the activities and subcellular distributions of creatine and adenylate kinases. J Neurochem 23:465–469

26. Maker HS, Lehrer GM, Silides DJ, Weiss C (1973) Regional changes in cerebellar creatine phosphate metabolism during late maturation. Exp Neurol 38:295–300

27. Bessman SP, Carpenter CL (1985) The creatine-creatine phosphate energy shuttle. Annu Rev Biochem 54:831–862